

# We are IntechOpen, the world's leading publisher of Open Access books Built by scientists, for scientists

6,900

Open access books available

185,000

International authors and editors

200M

Downloads

Our authors are among the

154

Countries delivered to

TOP 1%

most cited scientists

12.2%

Contributors from top 500 universities



WEB OF SCIENCE™

Selection of our books indexed in the Book Citation Index  
in Web of Science™ Core Collection (BKCI)

Interested in publishing with us?  
Contact [book.department@intechopen.com](mailto:book.department@intechopen.com)

Numbers displayed above are based on latest data collected.  
For more information visit [www.intechopen.com](http://www.intechopen.com)



# The Influence of Hybrid Aggregates on Different Types of Concrete

Jianhui Yang

## Abstract

This chapter presents different experimental results regarding the influences of normal-weight sand and lightweight sand (shale pottery (SP)) on different types of concrete. Because of the porosity of lightweight aggregates (LWAs), which can absorb and release water in concrete, the effect of concrete curing is better, and thus the properties of concrete are improved. On the other hand, because the lightweight coarse aggregate (LWCA) rises easily in all-lightweight concrete (ALWC) during pumping and vibration and the cost of ALWC is also higher, a method of replacing part of the lightweight aggregates in ALWC with normal-weight aggregates is used. These new types of concretes include sand lightweight concrete (SLWC), gravel lightweight concrete (GLWC), hybrid aggregate lightweight concrete (HALWC), and so on. This chapter mainly discusses the properties of lightweight aggregate concrete (LWAC), lightweight sand foamed concrete, lightweight sand mortar, and reinforced LWAC. The chapter also includes LWAC of high temperature, low temperature, durability, and uni- and multiaxial mechanical properties according to the results of our research group over recent decades. All of the experimental results show that the properties can meet Chinese National Code requirements.

**Keywords:** lightweight aggregate concrete, foamed concrete, mortar, reinforced concrete beam, durability, high temperature, low temperature, shale ceramsite, shale pottery

## 1. Introduction

There are notable differences between lightweight aggregates and normal-weight aggregates (NWA), so what are the different effects on different types of concrete?

Lightweight coarse aggregate has a softening effect; does lightweight aggregate concrete have this effect too?

Can the lightweight concrete be used under special environmental conditions such as negative temperature, elevated temperature, and chemical corrosion?

Are there any changes in the mechanical performance of lightweight concrete under complicated stress and in reinforced concrete?

Since 2005, it has been prohibited to mine river sand in most areas of China. The relevant laws, such as the *Water Law of the People's Republic of China* (2002, 2016),

the Flood Prevention Law of the People's Republic of China (1997, 2016), the Mineral Resources Law of the People's Republic of China (1986, 2009), and the Regulations of the People's Republic of China on the Administration of River Courses (1986, 2009), are constantly amended, and thus the prohibition of river sand excavation has been extended throughout the country since 2018. Nowadays, artificial sand is mainly used as normal-weight fine aggregate (NWFA) in normal-weight concrete (NWC) in China. This study mainly discusses artificial sand, and all of the following experiments were carried out strictly according to Chinese national standards.

## 2. Technical requirements of normal-weight sand

NWFA can be distinguished from lightweight fine aggregate (LWFA) by the apparent density ( $\rho_a$ ) and the bulk density ( $\rho_b$ ) [1, 2]. If  $\rho_a \geq 2500\text{kg/m}^3$  or  $\rho_b \geq 1400\text{kg/m}^3$  and the void ratio ( $e_v$ )  $\leq 44\%$  when calculated by Eq. (1), the sand is NWFA [1]. On the other hand, if  $\rho_b \leq 1200\text{kg/m}^3$ , the sand is LWFA. Also, the LWFA is usually made of lightweight coarse aggregate (LWCA) for producing lightweight aggregate concrete (LWAC) [2]:

$$e_v = \left(1 - \frac{\rho_b}{\rho_a}\right) \times 100\% \quad (1)$$

In order to standardise the artificial sand (AS), namely, manufactured sand (MS), the terms, definitions, classifications, specifications, technical requirements, test methods, inspection rules, and so on are stipulated in the Chinese national standards Sand for Construction (GB/T14684-2011) [1], Technical Specification for Application of Manufactured Sand Concrete (JGJ/T241-2011) [3], and Standard for Technical Requirements and Test Method of Sand and Crushed Stone (or Gravel) for Ordinary Concrete (JGJ52-2006) [4].

The MS is made of different parent rocks, whose strength should be in accordance with **Table 1** [3].

The fineness module ( $M_x$ , calculated by Eq. 2) should be  $M_{x,c} = 3.7-3.1$ ,  $M_{x,m} = 3.0-2.3$ ,  $M_{x,f} = 2.2-1.6$ , and  $M_{x,e} = 1.5-0.7$  for coarse, medium, fine, and extra-fine sand, respectively. The detailed particle size distribution sieved with a square hole mesh sieve is provided in **Table 2**:

$$M_x = \frac{(A_2 + A_3 + A_4 + A_5 + A_6) - 5A_1}{100 - A_1} \quad (2)$$

where  $A_1, A_2, A_3, A_4, A_5$  and  $A_6$  are the cumulative percentages retained in 4.75, 2.36, 1.18, 600, 300 and 150  $\mu\text{m}$  sieves, respectively.

For concrete production, it is recommended that sand from Zone II be used. The sand ratio (sand-to-sand and coarse aggregate weight ratio,  $S_p$ , %) should be improved properly when selecting sand from Zone I to keep a sufficient cement content to satisfy the workability requirement of concrete. When selecting sand from Zone III,  $S_p$  should be reduced properly. Also, medium sand should be selected

Igneous rock	Metamorphic rock	Sedimentary rock
$\geq 100$	$\geq 80$	$\geq 60$

Notes: The test method of compressive strength of parent rock refers to GB/T50266-2013 [5].

**Table 1.**  
Strength of parent rock made of artificial sand (unit, MPa).

Nominal diameter of sand and sieve hole	5 mm	2.5 mm	1.25 mm	630 μm	315 μm	160 μm	
Mesh size (length of sieve hole)	4.75 mm	2.36 mm	1.18 mm	600μm	300μm	150 μm	
Cumulative percentage retained (%)	Zone I	10–0	35 – 5	65–35	85–71	95–80	100–90
	Zone II	10–0	25–0	50 – 10	70–41	92–70	100–90
	Zone III	10–0	15–0	25–0	40–16	85–55	100–90

**Table 2.**  
 Particle size distribution for artificial sand stipulated in [1, 3].

for self-compacting concrete (SCC) production, and the percentage retained on a 315-μm sieve should not be less than 15%. The fineness modulus range of 2.6–3.0 is suitable for high-strength concrete (HSC) production. Moreover, medium sand should be used for mass concrete and mortar production [6].

### 3. Technical requirements of lightweight aggregate

Lightweight aggregate (LWA) includes artificial, natural, industrial waste slag, cinder, and spontaneous combustible coal gangue LWA [2]. LWA is called super-lightweight coarse aggregate (SLWCA) when  $\rho_b$  does not exceed 500 kg/m<sup>3</sup>. The tube crushing strengths (TCS) of the different grades of high-strength lightweight coarse aggregates (HSLWCAs) are provided in **Table 3**. The softening coefficient should be equal to or higher than 0.8 and 0.7 for artificial and industrial waste slag LWCA and natural LWCA, respectively. The fineness modulus ( $M_{x, LA}$ ) of LWFA should be between 2.3 and 4.0.

According to the current LWA production technology and its use in actual engineering, the particle size distribution of LWA is shown in **Table 4**.

Bulk density grade ( $\rho_b$ , kg/m <sup>3</sup> )	Tube crushing strength (MPa)	Strength grade of LWAC
600	4.0	LC25
700	5.0	LC30
800	6.0	LC35
900	6.5	LC40

Notes: The bulk density grade is a size range, not an exact number. For example,  $\rho_b = 600 \text{ kg/m}^3$  means  $500 < \rho_b < 600 \text{ kg/m}^3$  and so on.

**Table 3.**  
 Tube crushing strength and strength grade of LWAC for artificial HSLWCA stipulated in [2].

Mesh size (length of sieve hole)	4.75 mm	2.36 mm	1.18 mm	600μm	300μm	150 μm
Cumulative percentage retained (%)	0–10	0–35	20–60	30–80	65–90	75–100
Continuous grading (5–16 mm)	16.0 mm	9.50 mm	4.75 mm	2.36 mm		
Cumulative retained percentage (%)	0–10	20–60	90–100	95–100		
Continuous grading (5–10mm)	9.50 mm	4.75 mm	2.36 mm			
Cumulative percentage retained (%)	0 – 15	90–100	95–100			

**Table 4.**  
 Particle size distribution for LWFA and LWCA.

#### 4. Lightweight aggregate concrete

All-lightweight aggregate concrete (ALWAC), also known as all-lightweight concrete (ALWC), is made from LWFA, LWCA, cement, water, and other admixtures. Although ALWC has many excellent properties, such as high specific strength (ratio of cubic compressive strength to dry apparent density,  $SS$ ,  $\text{kN}\cdot\text{m}/\text{kg}$ ), high anti-deformability, excellent fire resistance, and so on, there are a number of negative aspects, such as low elastic modulus, the fact that LWCA rises more easily when pumping and vibrating LWAC, high costs, and so on. In order to satisfy the quality of both normal-weight concrete (NWC) and ALWC, new types of LWACs are formed by replacing parts of LWA with normal-weight aggregate (NWA) and vice versa. The naming rules are as follows.

The term 'ALWAC' was first mentioned in 1972 based on the available literature in the EI and SCI databases [7]. If, on the basis of ALWAC, only a part of LWFA is replaced with normal-weight sand in the same volume ratio  $S_S$  ( $\%$ ,  $0 < S_S \leq 100\%$ ), the LWAC is called sand lightweight concrete (SLWC) [7]. Similarly, if only a part of LWCA is replaced ( $0 < S_G \leq 100\%$ ) with normal-weight gravel, the concrete is called gravel lightweight concrete (GLWC). When both lightweight fine and coarse aggregates are replaced at the same time, the concrete is named hybrid aggregate lightweight concrete (HALWC). On the other hand, if on the basis of NWC, only a part of normal-weight coarse aggregate is replaced with expanded ceramsite ( $0 < S_C < 100\%$ ), the concrete is named hybrid aggregate concrete with less ceramsite (HACC). The other corresponding SCCs, fibre-reinforced concrete (FRC) and reinforced concrete (RC), obey the rules too.

Compared to ALWC and NWC, the abovementioned concrete can be uniformly named semi-lightweight concrete (semi-LWC), where the term 'semi' means the LWA is less than half, just half, or more than half in volume. But according to [8], the concrete is called LWAC when the dry apparent density of concrete ( $\rho_d$ ,  $\text{kg}/\text{m}^3$ ) is less than or equal to  $1950 \text{ kg}/\text{m}^3$ . Otherwise, it should be called specified density concrete (SDC) when  $1950 < \rho_d \leq 2300 \text{ kg}/\text{m}^3$ . The grade of dry apparent density is ranked from  $600$  to  $1900 \text{ kg}/\text{m}^3$ , the gradation is  $100 \text{ kg}/\text{m}^3$ , and the density range is  $\pm 50 \text{ kg}/\text{m}^3$ . For instance,  $\rho_d$  is  $600 \text{ kg}/\text{m}^3$  and the range is  $560\text{--}650 \text{ kg}/\text{m}^3$ .

In this study, the LWFA and LWCA are shale pottery (SP) and shale ceramsite (SC), while the NWFA and NWCA are MS or natural sand (NS, also known as river sand) and crushed stone (CS), respectively. Both LWCA and NWCA are crushed aggregates. The technical parameters of LWA and normal-weight aggregate (NWA) are listed in **Tables 5** and **6**, respectively.

The porosity of SC and SP is 51.3 and 23.9%, and the void ratio is 41.7 and 47.0% according to tests following GB/T17431.2-2010 [9], respectively. So the SC must be pre-wetted 24 hours (h) before production of concrete in order to prevent reabsorption of mixing water, because the water absorption rate ( $\%$ ,  $\omega_a$ ) is stable after 24 h, as shown in **Table 6**.

The ALWC is more sensitive to mix design than NWC mainly because of the higher porosity, lower bulk density, and lower tube crushing strength (TCS). Although the interface between crushed angular LWA and mortar is very good, the TCS is significantly lower compared to the mortar, and the LWCA floats more easily. The internal structure of ALWC becomes non-uniform, and thus the strength of ALWC depends on the strength of the mortar.

Many experiments have shown that the strength of ALWC mainly depends on the mass of the maximum diameter of LWCA, the mass of cementitious material (cement, fly ash (FA), silica fume, and other admixtures with gelling capacity), the water-to-binder weight ratio ( $W/B$ ), and the fine aggregate to overall aggregate weight ratio ( $\%$ ,  $S_p$ ) (42–47% in general).

SC	>16 mm (%)	16.0 mm (%)	9.50 mm (%)	4.75 mm (%)		
GB/T17431.1-2010	≤ 5	≤ 10	20-60	85-100		
Experimental values	0.1	1.6	34.2	99.7		
	Tube crushing strength (TCS) (MPa)			Mean	Over mean	GB/ T17431.1-2010
≥9.50 mm	3.63	3.67	3.68	3.66	3.62	2.0-3.0
≥4.75 mm	3.54	3.58	3.59	3.57		
SP	4.75 mm (%)	2.36 mm (%)	1.18 mm (%)	0.6 mm (%)	0.3 mm (%)	≤0.15 mm (%)
GB/T17431.1-2010	≤10	≤35	20-60	30-80	65-90	75-100
Experimental values	2.5	11.6	39.8	58.9	69.1	99.8
Gravel	>16 mm (%)	16.0 mm (%)	9.50 mm (%)	4.75 mm (%)	2.36 mm (%)	
GB/T 14685-2011	0	0-10	30-60	85-100	95-100	
Experimental values	0	8.4	48.6	92.3	98.7	
MS	4.75 mm (%)	2.36 mm (%)	1.18 mm (%)	0.6 mm (%)	0.3 mm (%)	≤0.15 mm (%)
GB/T 14684-2011	0-10	0-25	10- 50	41-70	70-92	80-94
Experimental values	7.8	24.6	47.2	66.9	89	93.7
NS	4.75 mm (%)	2.36 mm (%)	1.18 mm (%)	0.6 mm (%)	0.3 mm (%)	≤0.15 mm (%)
GB/T 14684-2011	0 - 10	0-25	10-50	41-70	70-92	90-100
Experimental values	6.5	21.4	37.9	63.9	89.9	97.9

Notes: The fineness module values of MS and NS are 3.06 and 2.98, respectively.

**Table 5.**  
 Technical parameters of LWA and NWA stipulated in the Chinese national standard and test values.

Diameter range (mm)	0.5 h	1 h	2 h	4 h	6 h	8 h	12 h	24 h	32 h	48 h	72 h
5-8	7.5	8.6	8.8	8.9	9.3	9.5	9.8	10.4	10.5	10.6	10.6
8-15	6.6	7.3	7.5	7.6	7.7	8.0	8.1	8.7	8.8	8.9	8.9

**Table 6.**  
 Water absorption rate ( $\omega_a$ ) of SC after different numbers of hours ( $h$ ).

Generally, the strength of NWC increases with curing time; however, the strength of ALWC decreases when the diameter of LWCA is larger than 20 mm. Because of that, the maximum diameter of LWCA should be 15 mm or smaller. On the other hand, the SC has a softening effect, the softening coefficient ( $\Psi_s$ ) stipulated in GB/T17431.1-2010 [2] is not less than 0.8, and increasing the maximum diameter leads to a decrease in  $\Psi_s$ . The test result is shown in **Table 7**, which can explain the difference in the strength forming mechanism between ALWC and NWC. Besides the abovementioned, when the maximum diameter of LWCA is larger, the damage area (area of LWCA versus mortar in a cross-section) is larger, so the strength of ALWC is lower; for example, the cubic compressive strength of ALWC is 32 MPa in 28 days, while the mortar strength after removing all LWCA in fresh concrete is 45 MPa.

Diameter range (mm)	7 d	14 d	28 d	60 d	90 d	120 d	180 d
$\Psi_{s1}$ (saturated surface dry condition)							
5–8	0.86	0.81	0.77	0.72	0.66	0.58	0.55
8–15	0.92	0.90	0.86	0.81	0.75	0.72	0.70
$\Psi_{s2}$ (oven dry condition)							
5–8	0.88	0.85	0.83	0.81	0.79	0.78	0.77
8–15	0.96	0.94	0.92	0.90	0.89	0.88	0.87

**Table 7.** Softening coefficient ( $\Psi_s$ ) of SC after soaking in water for different numbers of days ( $d$ ).

Type of concrete	$m_C$ (kg)	$m_{FA}$ (kg)	$m_{SC}$ (kg)	$m_{CS}$ (kg)	$m_{SP}$ (kg)	$m_{MS}$ (kg)	$m_W$ (kg)	$f_{cu}$ (MPa)	$f_c$ (MPa)	$f_{ts}$ (MPa)	$E_c$ (GPa)	$\rho_d$ (kg/m <sup>3</sup> )
ALWC	481	157	444	—	408	—	171	29.3	28.6	2.32	14.56	1594
SLWC			444	—	367	70		30.5	29.7	2.47	16.54	1612
GLWC			311	339	408	—		32.2	32.0	3.01	17.26	1796
HALWC			333	283	367	70		31.8	31.3	2.81	16.86	1785
HACC*	300	128	45	957	—	624	235	37.3	24.6	3.90	36.47	2280

Notes: (1)  $m_C$ ,  $m_{FA}$ ,  $m_{SC}$ ,  $m_{CS}$ ,  $m_{SP}$ ,  $m_{MS}$ , and  $m_W$  stand for cement (C), fly ash (FA), shale ceramsite (SC), crushed stone (CS), shale pottery (SP), manufactured sand (MS), and water (W), respectively; (2)  $f_{cu}$ ,  $f_c$ , and  $f_{ts}$  stand for the cubic compressive strength, axial compressive strength (prism specimen, height width ratio is 2 or 3), and splitting tensile strength (cubic specimen) at 28 days, respectively; (3)  $E_c$  is Young's elastic modulus; (4)  $\rho_d$  stands for dry apparent density; (5) HACC is the specified density concrete (SDC) judged by  $\rho_d$ .

\*HACC is the specified density concrete (SDC), the symbol of concrete strength grade can be expressed by "SC", which can be different from the symbol "C" of normal-weight concrete (NWC), and "LC" of lightweight aggregate concrete (LWAC).

**Table 8.** Reference mixes (1 m<sup>3</sup>) and test results of LWACs and SDC for LC30.

All of the following concretes are designed by pumping concrete; that is, the slump is 160–220 mm, mainly taking LC30, for example. The reference mixes and test results are shown in **Table 8**.

In **Table 8**, the cementitious material is PO<sub>4</sub>2.5 Portland cement and Grade II fly ash. The water reducing rate of high performance water reducing agent is not less than 20% and added 1.6–2.0 wt% (by mass of cementitious material).

Because of the difference of LWA and NWA, the strength, elastic modulus, and dry apparent density are increased when LWFA or LWCA is replaced separately by normal-weight aggregates, but it is more complex when replaced at the same time.

Also, the ratio ( $\zeta$ ) of axial compressive strength to cubic compressive strength for LWAC is usually close to 1.0, which is larger than the value of 0.66–0.67 required by JGJ51-2002 [6] and also larger than the value of 0.76 given for NWC. This phenomenon is precisely because the LWA with lower TCS will be crushed before the cement mortar and will show larger deformation, which is equivalent to antifricition and thus with self-lubricated capability.

#### 4.1 Autogenous shrinkage properties of LWACs

Because the hydration reaction of cement is an exothermic process, the amount of heat released leads to a temperature difference both inside and outside the concrete, and the temperature stress induces the appearance of cracks.

	ALWC	SLWC	GLWC	HALWC
Time (h)	31.0	34.0	36.0	27.5
Maximum temperature (°C)	66.4	63.9	62.4	65.5
Calculated temperature (°C)	66.1	69.7	59.5	53.5

**Table 9.**  
 Test and calculated values of adiabatic temperature rise for LWACs.

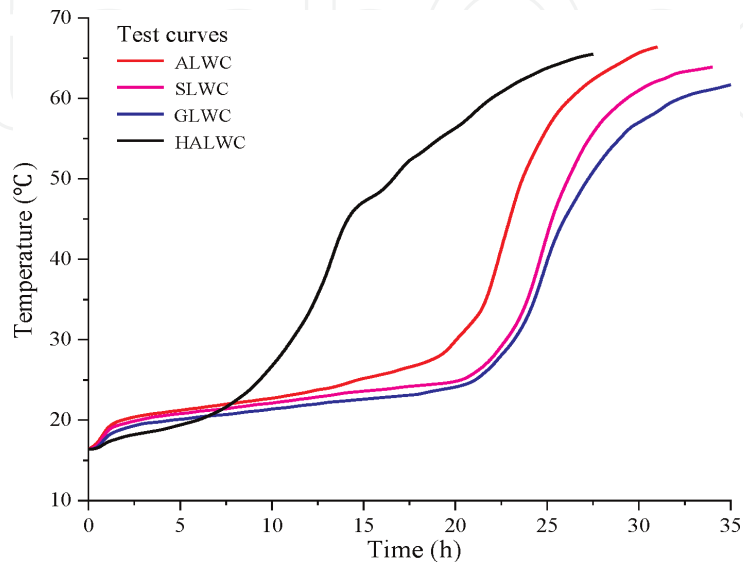


**Figure 1.**  
 Relationships between adiabatic temperature rise and time.

According to GB50496-2009 [6], the adiabatic temperature rise of LWACs is shown in **Table 9** (tested with a 3.7-litre Thermos bottle) and **Figure 1**.

Because the gas pressure in the Thermos bottle becomes higher as the hydration reaction proceeds, the Thermos glass liners burst at a certain time, as shown in **Table 9**. However, the length of time is shortest for HALWC. The reason may be the uniform distribution of normal-weight fine and coarse aggregates, which can improve the heat conduction rate and provide a better temperature distribution. On the contrary, the time period of the temperature rise is shorter for SC and SP compared to SLWC and GLWC, because of the higher porosity of LWA, which provides a better insulation performance. The difference between SLWC and GLWC may be that the distribution of NWFAs is more uniform than that of coarse aggregate, such as the sand particles touched in dot form can speed up heat conduction.

Autogenous shrinkage of concrete mainly happens after the initial setting time, but chemical shrinkage, which includes three complete stages, also has a significant influence. According to the mechanism of concrete shrinkage, chemical shrinkage happens because the absolute volume of hydration products is smaller than that of water and binding material during the early stage. Autogenous shrinkage happens during the skeleton structure forming in a later stage, so the unhydrated cement particles react further. In fresh concrete, the volume can also cause shrinkage because of the setting of parts of particles. Drying shrinkage is caused by water loss. In short, the cracks in concrete are mainly caused by plastic shrinkage in the early stage.

In **Figure 2**, the curves are smoothed after the peak values because of higher fluctuation (shown by dashed lines). The higher porosity and rougher surfaces of

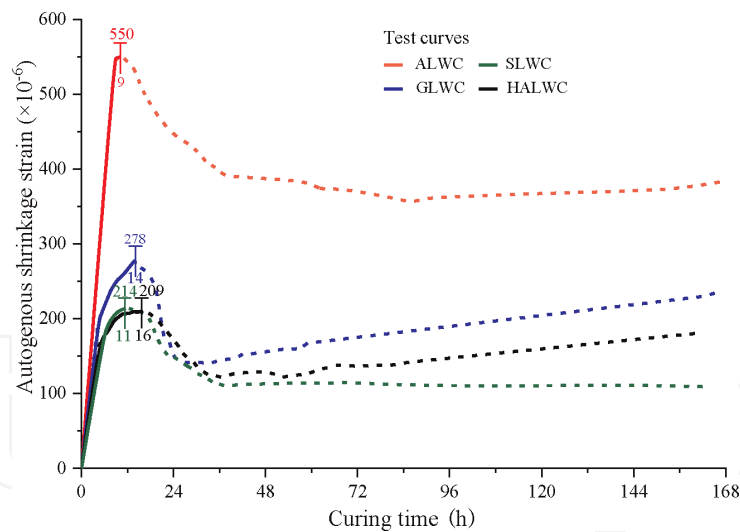


**Figure 2.**  
Test curves of autogenous shrinkage strain with time.

SC and SP also result in larger specific surface areas (total area of material per unit mass,  $m^2/g$ ), which can absorb more cement particles and thus improve hydration conduction, so the autogenous shrinkage of ALWC is greater in a shorter time period and then becomes stable. Among SLWC, GLWC, and HALWC, the autogenous shrinkage is mainly determined by the amounts of LWA. Because the specific surface area of aggregates is different, the internal distribution of aggregates is uniform, and parts of cement particles are subsident, which can determine the internal temperature stress field, so the resistance capability of plastic deformation is different.

## 4.2 Durability properties of LWACs

The effects of different mineral admixtures on the durability of LWACs were studied. **Table 10** shows the effects of substituting 75 wt% mineral powder (denoted as MP75; the activity index is 96% in 28 days) for fly ash and 50 wt% limestone powder (denoted as LP50), respectively. And both mineral powder and limestone powder are mixed in a ratio of 1:1, and total substitution for fly ash (marked MP75 + LP50) is based on **Table 8** (with a slight difference). The test method is according to GB50082–2009 [10].

Mineral powder can enhance both the strength and durability of concrete. Although the added limestone powder only reduces the strength of concrete, the requirements can be met, and the cost can be reduced. Because fly ash has become a scarce resource in China, mineral and limestone powder can be an effective alternative in the ready-mixed concrete industry.

Generally, the effects of normal-weight aggregates and mineral admixtures on carbonation and electric flux are not obvious, but according to GB50082-2009 [10], when the electric flux is between 1000 and 2000 C, the grade of chloride iron penetration is low, so the concretes can meet the requirements of the code.

## 4.3 Softening properties of LWACs

Since SC has a softening effect according to **Table 7**, is there also an SC concrete softening effect? The test results (**Table 11**) show that the LWACs almost have no softening effects. A possible reason is that the LWAs are strengthened because of their absorption of cement particles and hydration; on the other hand, the main contribution to the strength comes from the cement mortar, which does not show softening.

Type	$h_c^{28d}$ (mm)	$Q_e^{28d}$ (C)	$\Delta m^{21}$ (g)	$f_{cu}^{21}$ (MPa)	$f_{cu}^{28d}$ (MPa)	$K_f$ (%)
ALWC	12.6	1235	31.3	30.1	31.2	96.5
ALWC-MP <sub>75</sub>	10.8	1126	28.6	32.6	33.4	97.6
ALWC-LP <sub>50</sub>	11.8	1226	46.8	28.2	32.6	86.5
ALWC-MP <sub>50</sub> + LP <sub>50</sub>	—	—	33.7	29.8	34.7	85.9
SLWC	11.2	1126	32.6	36.6	38.6	94.8
SLWC-MP <sub>75</sub>	9.3	1042	31.6	38.1	40.6	93.8
SLWC-LP <sub>50</sub>	10.4	1092	43.1	34.3	39.4	87.1
SLWC-MP <sub>50</sub> + LP <sub>50</sub>	—	—	—	—	40.1	—
GLWC	10.2	1326	35.5	41.2	44.5	92.6
GLWC-MP <sub>75</sub>	8.3	1265	34.2	43.7	45.4	96.3
GLWC-LP <sub>50</sub>	9.5	1301	44.5	38.6	46.5	83.0
GLWC-MP <sub>50</sub> + LP <sub>50</sub>	—	—	—	—	46.1	—
HALWC	12.9	1410	34.7	36.9	39.7	92.9
HALWC-MP <sub>75</sub>	10.6	1339	33.5	38.3	40.8	93.9
HALWC-LP <sub>50</sub>	11.2	1389	46.3	35.2	40.5	86.9
HALWC-MP <sub>50</sub> + LP <sub>50</sub>	—	—	—	—	40.8	—
HACC	9.0	1007	—	36.4	38.3	95.0

Notes: (1)  $h_c^{28d}$  stands for the carbonation depth of concrete at 28 d; (2)  $Q_e^{28d}$  stands for electric flux after 6 h under chloride ion penetration of concrete at 28 d; (3)  $\Delta m^{21}$  and  $f_{cu}^{21}$  stand for the mass loss and cubic compressive strength of concrete after 21 dry-wet cycles under sulphate attack, respectively; (4) the test is stopped when the ratio of  $K_f = f_{cu}^{21}/f_{cu}^{28d} \times 100\%$  is larger than 75% according to GB50082–2009 [10].

**Table 10.**  
 Test results of durability for different LWACs and SDC with LC<sub>30</sub>.

**Table 11** shows that the concrete strength and elastic modulus increase under curing in water on different days. However, the HALWC falls slightly, and the elastic modulus is almost constant. Similarly, for any type of LWAC, all of the  $\zeta$  values are also close to 1.0 on different days.

The test results show the LWACs are without a softening effect, so they can be used in hydraulic structure engineering and underground engineering.

#### 4.4 Properties of LWACs after elevated temperature treatment

The appearance characteristics and strength of LWACs are shown in **Tables 12** and **13** under different temperatures ( $T$ , °C), respectively. When the temperature is below 200°C, the surface of concrete shows no change, and the strength increases, but when the temperature is above 300°C, changes in both colour and crack shape can be observed. The maximum width of cracks ( $w_{max}$ , mm) increases with increases in temperature and the strength decreases.

Although the mass loss in different types of concretes shows no obvious difference after high-temperature treatment, the effect of the addition of NWAs alone on the strength and elastic modulus is higher and changes regularly; that is, added NWCA alone larger than added NWFA alone, but smaller when added at same time than added NWCA only.

In general, the residual values of elastic modulus are larger than those of strength, which means the anti-deformation capacity of concrete decreases with

	Type	28 d	60 d	90 d	120 d	180 d	$\psi_c$ (%)
$f_{cu}$ (MPa)	ALWC	30.98	31.54	31.05	30.15	29.78	101.3
	SLWC	31.48	32.43	31.87	31.44	31.20	100.9
	GLWC	34.43	35.18	35.09	34.92	34.81	102.8
	HALWC	33.56	34.22	33.96	33.68	33.47	102.5
$f_c$ (MPa)	ALWC	29.45	30.27	29.81	28.95	28.07	99.9
	SLWC	30.87	31.56	30.78	30.49	30.15	100.6
	GLWC	33.59	34.14	33.96	33.75	33.62	102.7
	HALWC	31.35	32.84	32.61	32.39	32.18	102.9
$f_{ts}$ (MPa)	ALWC	2.96	3.03	2.95	2.86	2.79	104.5
	SLWC	3.04	3.11	3.03	2.95	2.90	104.3
	GLWC	3.15	3.23	3.20	3.18	3.15	104.3
	HALWC	3.07	3.19	3.14	3.11	3.09	105.1
$E_c$ (GPa)	ALWC	21.23	21.74	22.35	23.24	23.79	115.2
	SLWC	21.62	22.24	22.85	23.41	23.98	115.3
	GLWC	21.92	22.80	23.35	23.96	24.71	116.4
	HALWC	21.58	22.45	23.09	23.62	24.35	116.3

Notes:  $\psi_c$  stands for the softening coefficient of concrete.

**Table 11.**

Test results of LWACs with LC30 under water curing on different days.

$T$ (°C)	Colour	Visible phenomenon	$w_{max}$ (mm)			
			ALWC	SLWC	GLWC	HALWC
300	Light grey	Fewer hairline cracks	0.06	0.04	0.05	0.04
400	Off-white	More hairline cracks	0.16	0.12	0.14	0.12
500	Hazel	Honeycomb cracks	0.20	0.20	0.20	0.18
600	Brownness	Honeycomb cracks with surface wrapping	0.30	0.26	0.28	0.24

**Table 12.**

Appearance characteristics of LWACs after high-temperature treatment.

rises in temperature. On the other hand, the residual strengths of LWACs after high-temperature treatment are very close to or even higher than that of NWC, which indicates that LWACs can be used for fire-resistant design. For example, the residual strength of axial compression is 95% at 200°C, 80–90% at 300°C, 70–75% at 400°C, 60–65% at 500°C, and around 50% at 600°C. The residual splitting tensile strength is around 90%, 75–80%, 60–65%, 50–55%, and around 45% at 200, 300, 400, 500, and 600°C, respectively.

#### 4.5 Properties of LWACs cured at negative temperature

During the construction process used by the artificial freezing method, the ambient temperature in the working place is from  $-8$  to  $-12^\circ\text{C}$  in China. Concrete properties after curing at negative temperature are shown in **Tables 14** and **15**, where the specimen is wrapped with a layer of quilt after being poured and then put into a low-temperature test chamber.

	Type	200°C	300°C	400°C	500°C	600 °C	$\eta_c^T$ (%)
$\Delta m$ (%)	ALWC	1.1	4.5	5.4	6.4	7.0	
	SLWC	1.3	4.6	5.6	6.7	7.2	
	GLWC	0.9	4.2	4.7	5.5	6.8	
	HALWC	0.8	4.2	4.9	5.8	6.9	
$f_{cu}$ (MPa)	ALWC	30.54	25.70	22.02	19.79	16.48	55.9
	SLWC	32.05	28.98	25.01	21.35	17.22	56.4
	GLWC	33.23	32.25	25.86	23.05	18.34	57.0
	HALWC	32.65	31.82	25.14	22.21	17.90	56.8
$f_c$ (MPa)	ALWC	26.88	23.43	20.04	17.50	14.68	52.0
	SLWC	26.76	25.31	21.82	18.90	15.12	50.9
	GLWC	29.77	26.96	23.19	19.14	15.95	50.9
	HALWC	28.51	26.92	22.65	18.51	14.82	48.1
$f_{ts}$ (MPa)	ALWC	2.06	1.79	1.46	1.25	1.07	46.1
	SLWC	2.22	1.93	1.59	1.36	1.14	46.2
	GLWC	2.73	2.40	1.96	1.69	1.47	48.8
	HALWC	2.53	2.25	1.80	1.55	1.35	48.0
$E_c$ (GPa)	ALWC	12.61	10.13	8.19	6.62	5.03	34.5
	SLWC	15.68	13.75	10.98	8.88	6.13	37.1
	GLWC	16.89	16.46	14.53	11.19	8.76	50.8
	HALWC	16.11	15.32	13.65	10.11	8.12	48.2

Notes:  $\Delta m$  stands for the ratio of mass after high-temperature treatment to that under room temperature.  $\eta_c^T$  stands for the ratio of strength or elastic modulus at 600°C to that at room temperature.

**Table 13.**  
 Test results of LWACs for LC30 after elevated temperature treatment.

The compressive strength and elastic modulus of the specimens cured at  $-5^\circ\text{C}$  meet the basic requirements (up to 90%) both with and without anti-freezing agent, but at  $-10^\circ\text{C}$ , they can satisfy the requirements when added anti-freezing agent.

Although the strength and elastic modulus of other groups fail the basic requirements, the hydration reaction does not stop but only diminishes. Compared with NWC, the strength of the specimen is higher, which shows that it helps promote the hydration reaction because of the heat preservation and inner curing effect of LWA. On the other hand, the strength of GLWC is slightly higher than that of ALWC under the same conditions. The reason is the same as the one mentioned above, namely, that the elastic modulus of gravel is larger than that of ceramsite.

Also, fibre can enhance the strength and elastic modulus of specimens cured at negative temperature, and the laws are also the same; that is, the performance of concrete is better with elastic modulus of fibre increasing.

To summarise, the LWACs can meet the requirements of freezing process construction.

#### 4.6 Uniaxial stress-strain curves of LWACs

The uniaxial stress-strain curve of LWACs is similar to that of NWC, as shown in **Figure 3**, but the total strain of LWACs is significantly larger than that of NWC.

T (°C)	w <sub>A</sub> (%)	ALWC, f <sub>cu</sub> (MPa)						η <sub>c</sub> <sup>T</sup> (%)	GLWC, f <sub>cu</sub> (MPa)				η <sub>c</sub> <sup>T</sup> (%)
		1 d	2 d	3 d	7 d	14 d	28 d		3 d	7 d	14 d	28 d	
-5	0	4.9	11.3	16.5	20.5	24.7	29.3	90.1	16.9	21.1	26.0	31.3	90.9
	2	6.2	12.5	17.9	27.3	—	32.1	98.7	—	—	—	—	—
-10	0	4.1	10.8	13.8	17.5	21.4	25.0	76.9	14.4	18.9	23.3	27.2	79.0
	2	5.8	12.1	16.1	24.4	—	29.7	91.3	—	—	—	—	—
-15	0	37	8.5	10.3	13.3	15.8	18.6	57.2	11.4	14.3	17.5	20.7	60.1
	3	5.3	11.8	15.4	18.9	—	27.5	84.6	—	—	—	—	—

Notes: (1) w<sub>A</sub> stands for the ratio of anti-freezing agent to cement (by mass); (2) η<sub>c</sub><sup>T</sup> stands for the ratio of strength at 28 days and curing at negative temperature to that at room temperature; (3) the mixes are slightly different from Table 8.

**Table 14.** Compressive strength of LWACs cured at negative temperature with anti-freezing agent for LC30.

T (°C)	ALWC, f <sub>c</sub> (MPa)				η <sub>c</sub> <sup>T</sup> (%)	GLWC, f <sub>c</sub> (MPa)				η <sub>c</sub> <sup>T</sup> (%)
	3 d	7d	14 d	28 d		3 d	7d	14 d	28 d	
-5	14.46	18.41	22.36	24.63	83.0	15.81	20.34	24.64	26.45	85.0
-10	12.65	16.16	19.63	21.34	71.9	14.86	17.87	21.98	23.34	75.0
-15	10.88	13.18	15.54	16.62	56.0	11.94	14.49	17.21	18.15	58.3
	f <sub>ts</sub> (MPa)					f <sub>ts</sub> (MPa)				
-5	1.87	2.49	3.03	3.42	91.9	2.03	2.54	3.13	3.49	92.3
-10	1.69	2.15	2.71	2.99	80.4	1.83	2.30	2.75	3.06	81.0
-15	1.50	1.88	2.21	2.46	66.1	1.69	1.97	2.32	2.55	67.5
	E <sub>c</sub> (GPa)					E <sub>c</sub> (GPa)				
-5	9.43	13.22	16.49	18.77	92.0	10.02	14.23	17.56	19.36	94.0
-10	8.81	12.58	15.03	16.52	81.0	8.97	12.01	14.98	17.10	83.0
-15	8.26	11.57	13.61	14.28	70.0	8.44	11.15	13.22	15.04	73.0

**Table 15.** Test results of LWACs cured at negative temperature without anti-freezing agent for LC30.

The symbols of stress and strain obey the following rules: the plus sign ‘+’ denotes tension; the minus sign ‘-’ denotes compression.

Generally, the stress-strain curve can be expressed by Eqs. (3) and (4) [11].

Ascending curve:

$$y = \alpha x + (3-2\alpha)x^2 + (\alpha-2)x^3 \quad x \leq 1 \quad (3)$$

Descending curve:

$$y = \frac{x}{\beta(x-1)^2 + x} \quad x \geq 1 \quad (4)$$

where  $x = \frac{\varepsilon}{\varepsilon_0}$  and  $y = \frac{\sigma}{\sigma_0}$ .  $\alpha$  and  $\beta$  are fitting coefficients shown in Table 16.  $\varepsilon_0$  and  $\sigma_0$  stand for peak strain and peak stress under uniaxial compression, respectively.

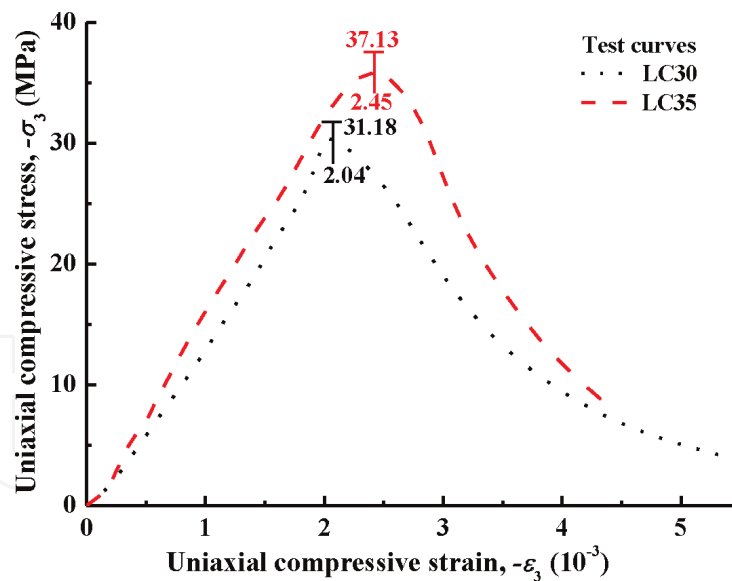


**Figure 3.**  
 Test curves of stress-strain under uniaxial compression for ALWC.

Strength grade	Ascending curve		Descending curve	
	$\alpha$	$R^2$	$\beta$	$R^2$
LC 30	-0.3777	0.9332	4.7704	0.9921
LC 35	0.4398	0.9855	9.0217	0.9975

**Table 16.**  
 Fitting coefficients and relative coefficients in Eqs. (3) and (4).

Eqs. (3) and (4) can be fitted for all kinds of concretes, whether or not the curve is complete. In particular, direct measurement of the descending curve is not usually easy (**Figure 4**).

Although **Figure 4** does not contain descending curves, the law of different LWACs is the same; that is, the ultimate stress decreases, and the ultimate strain increases with the temperature increase, which shows that the plastic deformation gets larger because the strength of the cement mortar matrix decreases. On the other hand, under the same temperature, the effects of a small quantity of NWA on the ultimate strain are not significant; only the effect on the ultimate stress is remarkable. At the same time, ALWC is similar to SLWC, and GLWC is similar to HALWC.

#### 4.7 Multiaxial strength of LWACs

Under multiaxial compressive stresses, the ultimate compressive strength of concrete will increase significantly, and therefore the failure modes change. For example, ALWC undergoes the phenomenon of squeeze flow, and a plastic plateau appears in the stress-strain curve under the two larger lateral stresses.

**Tables 17** and **18** show the bi- and triaxial ultimate compressive strengths tested by a large real triaxial test system, respectively. To reduce the friction, a two-layer polythene film with lithium base oil smeared between the layers is used, which can guarantee that the strength under single stress action ( $\sigma_0$ ) is close to the axial compressive strength ( $f_c$ ). In the test,  $\sigma_0$  is slightly smaller than  $f_c$ , and the loading type is proportional loading. The samples were tested after 120 days of curing.

The formulas for calculating bi- and triaxial ultimate strength are shown as Eqs. (5) and (6) [12], respectively:

$$\sigma_3 = \frac{1 + \omega_2}{1 + \omega_2^{-1}} \sigma_2, \omega_2 = \frac{\sigma_3}{\sigma_2} \quad (5)$$

$$\sigma_3 = \frac{\sqrt{\sigma_1 \sigma_2 (1 + \omega_1 + \omega_3) (1 + \omega_2 + \omega_3^{-1})}}{1 + \omega_1^{-1} + \omega_2^{-1}} \omega_1 = \frac{\sigma_3}{\sigma_1}, \omega_3 = \frac{\sigma_2}{\sigma_1} \quad (6)$$

The smaller relative error indicates that the test data are reliable and the formulas are correct. On the other hand, the multiaxial ultimate strength increases with

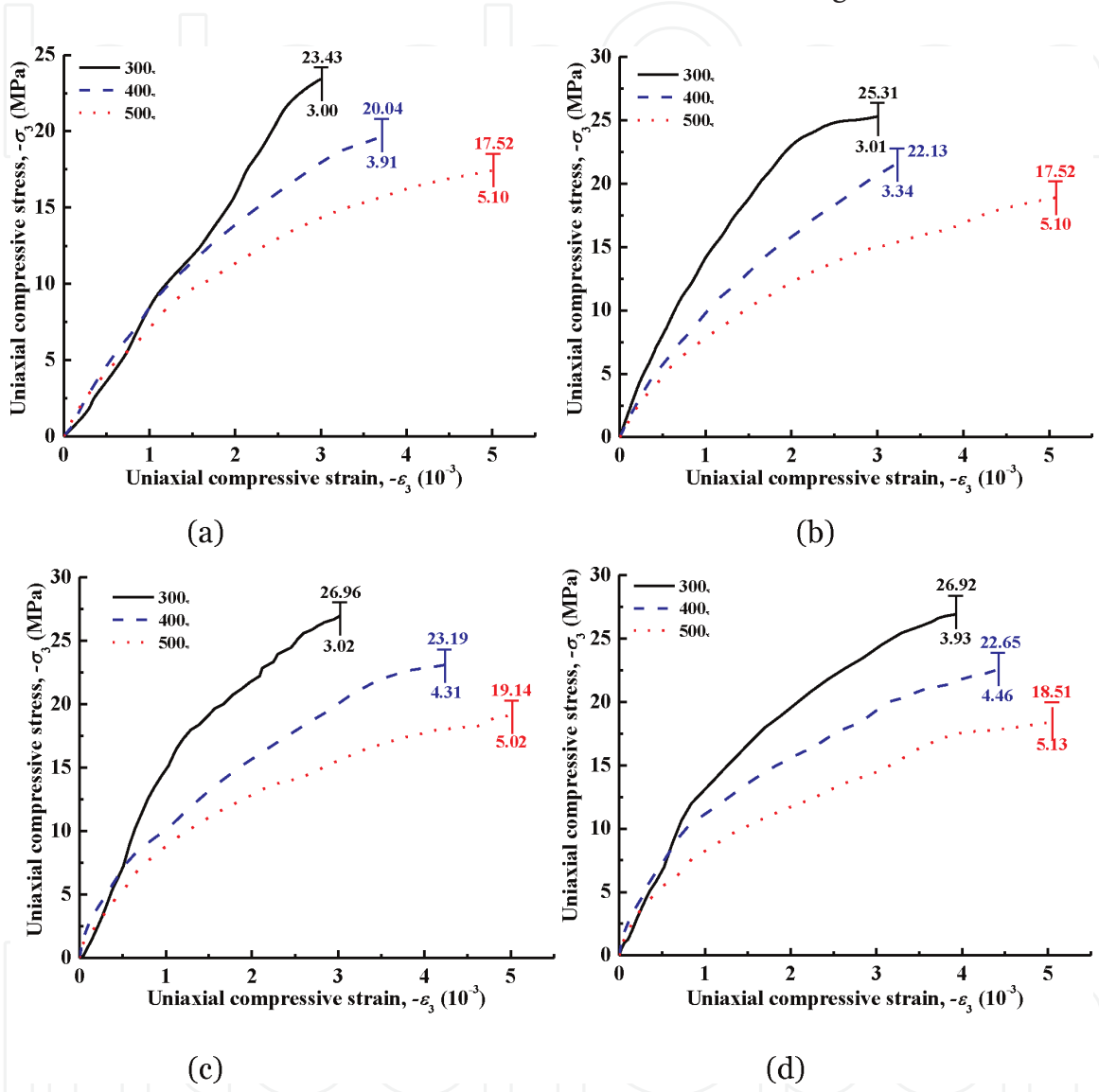


**Figure 4.** Test curves of stress-strain under uniaxial compression for LWACs after elevated temperature treatment. (a) ALWC, (b) SLWC, (c) GLWC, and (d) HALWC.

$\sigma_3:\sigma_2$	$-\sigma_{30}$ (MPa)	Eq. (5) (MPa)	$E_r$ (%)	$\sigma_{30} / f_c^{120 d}$
1:0.25	40.94	-42.62	4.10	1.28
1:0.5	39.92	-41.75	4.58	1.24
1:0.75	39.88	-41.96	5.22	1.25
1:1	41.88	-44.28	5.73	1.31

Notes: (1)  $\sigma_{30}$  stands for peak stress, namely, ultimate compressive strength.  $E_r$  stands for relative error.

**Table 17.** Biaxial compressive strength under proportional loading.

$\sigma_3:-\sigma_2:-\sigma_1$	$-\sigma_1$ (MPa)	$-\sigma_2$ (MPa)	$-\sigma_3$ (MPa)	Eq. (6) (MPa)	$E_r$ (%)	$\sigma_{30} / f_c^{120 d}$
1:0.1:0.1	5.11	4.98	49.77	-51.1	2.6	1.56
1:0.25:0.25	19.58	19.10	75.85	-78.32	3.2	2.37
1:0.5:0.5	50.61	49.21	97.94	-101.22	3.3	3.06
1:1:0.1	6.48	60.81	60.51	-64	5.7	1.89
1:1:0.25	22.56	87.03	86.48	-90.24	4.3	2.70
1:1:0.5	55.61	107.37	106.78	-111.22	4.1	3.34
1:0.25:0.1	7.56	36.62	58.62	-60.60	3.3	1.83
1:0.5:0.1	19.04	30.98	72.85	-75.80	4.1	2.28
1:0.5:0.25	6.06	14.77	73.64	-76.16	3.4	2.30

**Table 18.**  
 Triaxial compressive strength under proportional loading.

increasing lateral stress; the law is the same as for NWC, but the ratio of  $\sigma_{30}$  to  $f_c$  is larger than that of NWC. Also, the stress-strain curves show that the deformation resistance capacity of LWACs is stronger than that of NWC, so the LWACs cannot be crushed easily and thus have higher strength under the action of multiaxial stress.

The ultimate strength and elastic modulus of LWACs under traditional triaxial stresses are shown in **Table 19**.

All of the strength and elastic modulus values increase with increasing confining pressure. Under the same temperature and confining pressure, the effect on NWA is highest when using the lowest amount of hybrid aggregate, such as gravel, NS, and LWS. However, when the temperature is above 300°C, the strength of HALWC is smaller than those of SLWC and GLWC. At the same time, below 300 °C, the strength increases, except for HALWC, whose strength increases at temperatures below 200°C. The relationship between ultimate compressive strength and confining pressure can be expressed by Mohr-Coulomb theory as shown in Eq. (7).

	$T$ (°C)	-2 MPa	-4 MPa	-6 MPa	-8 MPa	-10 MPa
ALWC $-\sigma_{30}$ (MPa)	20	29.30	32.92	35.25	39.29	43.23
	200	31.04	37.45	42.98	48.10	51.86
	300	26.96	31.57	37.55	40.89	44.76
	400	22.15	27.30	32.77	38.14	40.83
	500	25.90	27.04	30.58	32.57	36.26
SLWC $-\sigma_{30}$ (MPa)	20	31.06	34.23	37.97	39.49	44.50
	200	36.36	40.56	43.54	45.90	50.27
	300	40.76	42.41	49.27	51.07	53.70
	400	30.80	33.48	39.63	43.33	48.22
	500	30.66	32.73	37.52	42.04	43.74
GLWC $-\sigma_{30}$ (MPa)	20	37.44	44.89	49.84	55.19	59.23
	200	40.59	47.56	51.44	57.85	62.10
	300	41.08	47.51	54.31	60.44	63.99
	400	34.74	40.07	45.90	46.66	54.76
	500	30.91	35.71	38.59	45.81	49.18

	T (°C)	-2 MPa	-4 MPa	-6 MPa	-8 MPa	-10 MPa
HALWC $-\sigma_{30}$ (MPa)	20	34.73	40.61	45.47	52.27	53.87
	200	43.34	45.55	49.35	55.42	59.59
	300	42.51	43.42	46.14	50.83	53.79
	400	30.84	37.71	42.13	47.56	51.81
	500	26.55	31.24	37.63	43.07	49.63
ALWC $E_c$ (GPa)	20	10.74	11.03	11.21	12.86	14.15
	200	10.94	11.62	13.31	13.82	14.36
	300	6.29	7.64	7.51	8.19	11.12
	400	5.25	6.64	6.86	7.65	7.78
	500	4.97	5.37	6.13	6.23	6.37
SLWC $E_c$ (GPa)	20	9.80	10.43	10.56	12.42	14.52
	200	12.21	12.83	13.22	13.70	14.83
	300	10.72	10.89	12.26	12.75	14.35
	400	7.27	8.53	8.67	8.72	8.80
	500	6.80	6.93	7.69	7.89	8.21
GLWC $E_c$ (GPa)	20	10.86	11.56	13.23	14.62	15.75
	200	9.10	13.36	13.76	14.35	14.47
	300	10.95	11.12	13.66	13.75	14.01
	400	8.55	8.86	8.90	9.83	9.97
	500	7.01	7.23	7.54	7.45	8.15
HALWC $E_c$ (GPa)	20	11.18	13.70	14.12	14.78	15.90
	200	11.80	12.33	12.55	14.01	15.09
	300	10.98	12.01	12.31	13.96	14.19
	400	7.78	8.84	8.93	9.81	9.82
	500	6.69	7.27	8.13	8.24	8.84

Notes: The values of confining pressure are 2, 4, 6, 8, and 10 MPa, respectively.

**Table 19.**

Test results of LWACs under traditional triaxial compression after elevated temperature treatment for LC30.

$$\frac{\sigma_{30}}{f_c} = 1 + C \left( \frac{\sigma_1}{f_c} \right)^c \quad \sigma_1 = \sigma_2 \quad (7)$$

where  $C$  and  $c$  are the fitting coefficients for each temperature group and concrete group, respectively.

The absolute values of relative error are all smaller than 5%.

## 5. Properties of lightweight sand foamed concrete

In China, traditional foamed concrete generally consists of cement, NS, water, foam agent, and so on [13, 14]. Because the densities of cement and NS are significantly higher than the density of water, these particles sink easily and therefore

Type	$m_C$ (kg)	$m_{FA}$ (kg)	$m_{SP}$ (kg)	$m_{SC}$ (kg)	$m_W$ (kg)	$m_F$ (g)	$f_{cu}^{28d}$ (MPa)	$\rho_d$ (kg/m <sup>3</sup> )	$\lambda$ (w/(m.k))
LFC 5	230	130	430	110	112	407	5.2	973	0.12
LFC 10	260	145	520	130	126	370	12.1	1185	0.26
LFC 20	360	198	543	136	173	280	24.5	1410	0.35
LFC 30	360	235	630	220	184	208	33.1	1723	0.42

Notes:  $m_F$  stands for the mass of foam agent.

**Table 20.**  
 Reference mixes (1 m<sup>3</sup>) and test results of all-lightweight foamed concrete.

cause the foamed concrete to crack. According to the properties, the bulk density of LWA is smaller than that of water, and thus the foamed concrete consists of LWA foamed by physical foaming, which can be called all-lightweight foamed concrete (ALWFC). It does not crack and also makes a higher-strength-grade concrete (up to LFC 30; LFC is the code name of strength grade of mortar). Because of these properties, it can be widely used in non-structure and structure concrete and pumped but not vibrated. The LWAs are SC and SP in foamed concrete in this study, and the mixes are shown in **Table 20**.

Although there are countless air pores in ALWFC, most of these pores are discontinuous, so ALWFC has better durability. According to the test results, the carbonation depth generally does not exceed 5 mm in 56 days, and the resistance performance with regard to chloride ion permeability, that is, the electric flux after 6 hours, is smaller than 1000 C. On the other hand, the ALWFC also has better fire resistance, sound insulation, and sound absorption capabilities.

## 6. Properties of reinforced ALWC

Taking a reinforced ALWC beam, for example, the parameters of the tested beams are shown in **Tables 21–25** and **Figures 5** and **6**.

The test results according to GB50152-2012 [15] are as follows.

According to [16, 17], during the beam flexural test, the maximum crack width should not exceed 0.3 mm under service loads, and the deflection should not exceed  $l_0/200 = 10.5$  mm. The test values are 0.27 and 5.21 mm for the crack width and deflection, respectively, so ALWC can meet the code requirements. On the other hand, the crack load is about 28% of the ultimate load, and the service load is about 72%; these values are basically the same as those for the RC beam.

For the shear beam, because there is no warning before the occurrence of diagonal cracks, the diagonal cracks occur in the shear span section when the load is 20% of the ultimate load and then rapidly expand to the length of 100–150 mm. The initial width of the diagonal crack is generally 0.05 mm in the reinforced NWC beam compared to 0.03 mm in this study. At the same time, the maximum width of cracks and the deflection under service loads are 0.29 mm and 10.05 mm, respectively, thus meeting the code requirements.

The theoretical and test values of ultimate strength for normal and diagonal sections are shown in **Table 25**. All the test values slightly exceed the theoretical values. Compared to a reinforced NWC beam with the same stiffness, the width and height of the cross-section need to be increased by 18%, respectively. On the other

No.	$b \times h$ (mm)	$h_0$ (mm)	$l_0$ (mm)	$\lambda$	Longitudinal tension bars			Stirrup	
					Bar	$A_s$ (mm <sup>2</sup> )	$\rho_s$ (%)	Bar	$\rho_{sv}$ (%)
B1	150 × 300	267	2100	—	2 $\ominus$ 16	402	1.00	$\Phi$ 8@100	0.67
B2	150 × 300	270	2100	—	2 $\ominus$ 10	157	0.39	$\Phi$ 8@100	0.67
B3	150 × 300	264	2100	—	3 $\ominus$ 22	1140	2.89	$\Phi$ 8@100	0.67
S4	150 × 300	267	2100	2	2 $\ominus$ 16	402	1.00	$\Phi$ 8@140	0.48
S5	150 × 300	270	2100	2	2 $\ominus$ 10	157	0.39	$\Phi$ 8@140	0.48
S6	150 × 300	265	2100	2	2 $\ominus$ 20	628	1.58	$\Phi$ 8@140	0.48
S7	150 × 300	267	2100	0.95	2 $\ominus$ 16	402	1.00	$\Phi$ 8@140	0.48
S8	150 × 300	267	2100	1.5	2 $\ominus$ 16	402	1.00	$\Phi$ 8@140	0.48
S9	150 × 300	267	2100	3.05	2 $\ominus$ 16	402	1.00	$\Phi$ 8@140	0.48
S10	150 × 300	267	2100	2	2 $\ominus$ 16	402	1.00	$\Phi$ 8@140	0.48
S11	150 × 300	267	2100	2	2 $\ominus$ 16	402	1.00	$\Phi$ 8@100	0.67
S12	150 × 300	267	2100	2	2 $\ominus$ 16	402	1.00	$\Phi$ 8@180	0.37

Notes: (1) The notations 'B' and 'S' stand for bend and shear, respectively; (2)  $b$  and  $h$  stand for the width and height of a beam cross, respectively; (3)  $l_0$  stands for the calculated span; (4)  $\lambda$  stands for the ratio of shear span to effective depth; (5)  $\ominus$  and  $\Phi$  stand for hot rolled crescent-shaped bars (HRCSB, hereinafter referred to as crescent ribbed bars, CRB) and hot rolled plain steel bars (HRPSB, hereinafter referred to as plain steel bars, PSB), respectively; (6)  $A_s$  stands for transverse area; (7)  $\rho_s$  and  $\rho_{sv}$  stand for the ratio of reinforcement and ratio of stirrup reinforcement, respectively; (8) @ stands for the spacing between stirrups; (9) the diameter of a steel bar means the nominal diameter ( $d$ ), and the concrete is ALWC with LC30; (10) each of the test beams has two hanger bars (2 $\ominus$ 12) in order to meet detailing requirements.

**Table 21.**  
Parameters of test beams for bend and shear, respectively.

Type	$d$ (mm)	$f_y$ (MPa)	$f_u$ (MPa)	$E_s$ (MPa)
PSB	8	316	434	$2.1 \times 10^5$
	10	329	457	$2.0 \times 10^5$
	12	335	482	$2.0 \times 10^5$
CRB	16	342	527	$2.0 \times 10^5$
	18	362	576	$2.0 \times 10^5$
	22	396	612	$2.0 \times 10^5$

Notes:  $f_y$  stands for yield strength;  $f_u$  stands for ultimate tensile strength.

**Table 22.**  
Parameters of PSB and CRB.

hand, if the section remains unchanged, according to the numerical simulation results for a seven-storey residential building, the total weight of the building is reduced by around 14.8%, and the inter-storey displacement angle is increased by

around 27.5% under earthquake loading. This is because ALWC has a bigger ratio of cubic compressive strength to dry apparent density, a smaller elastic modulus, and a larger anti-deformation capacity.

No.	Cracking load and maximum width of crack		Service load and maximum width of crack		Failure load and maximum width of crack	
	$P_{cr}$ (kN)	$w_{cr, max}$ (mm)	$P_k$ (kN)	$w_{k, max}$ (mm)	$P_u$ (kN)	$w_{u, max}$ (mm)
B1	30	0.11	70	0.24	100	1.85
B2	15	0.15	35.7	0.27	51	1.54
S4	45	0.14	120.5	0.19	160	0.63
S5	30	0.01	130.9	0.22	187.1	0.43
S6	25	0.02	129.7	0.25	185.3	0.41
S7	45	0.01	145.3	0.28	207.5	0.57
S8	40	0.012	135.9	0.29	194.1	0.63
S9	30	0.013	119.5	0.26	170.7	0.50
S10	35	0.017	139.0	0.26	198.6	0.56
S11	42	0.019	166.3	0.21	237.5	0.49
S12	30	0.01	115.2	0.21	164.6	0.43

**Table 23.**  
 Maximum crack widths under different load stages.

No.	Yield load and deflection		Ultimate load and deflection	
	$P_y$ (kN)	$\delta_y$ (mm)	$P_u$ (kN)	$\delta_u$ (mm)
B1	85	5.21	100	29.6
B2	43.4	4.11	51	19.75
B3	—	—	160	5.63
S4	150.3	9.52	187.1	29.76
S5	140.5	9.51	185.3	29.53
S6	165.4	8.87	189.6	29.89
S7	180.6	9.02	207.5	23.87
S8	145.3	9.24	194.1	29.79
S9	115.8	10.05	170.7	27.82
S10	150.5	9.41	198.6	28.42
S11	175.9	9.53	237.5	29.92
S12	125.2	9.76	164.6	28.57

**Table 24.**  
 Deflections under yield and ultimate load, respectively.

No.	$f_c$ (MPa)	$f_y$ (MPa)	$A_s$ (mm <sup>2</sup> )	$h_0$ (mm)	$b$ (mm)	$M_u^c$ (kN·m)	$M_u^t$ (kN·m)	$M_u^t/M_u^c$
B1	31.80	342	402	267	150	34.73	35	1.01
B2	30.51	329	157	270	150	13.65	17.85	1.30

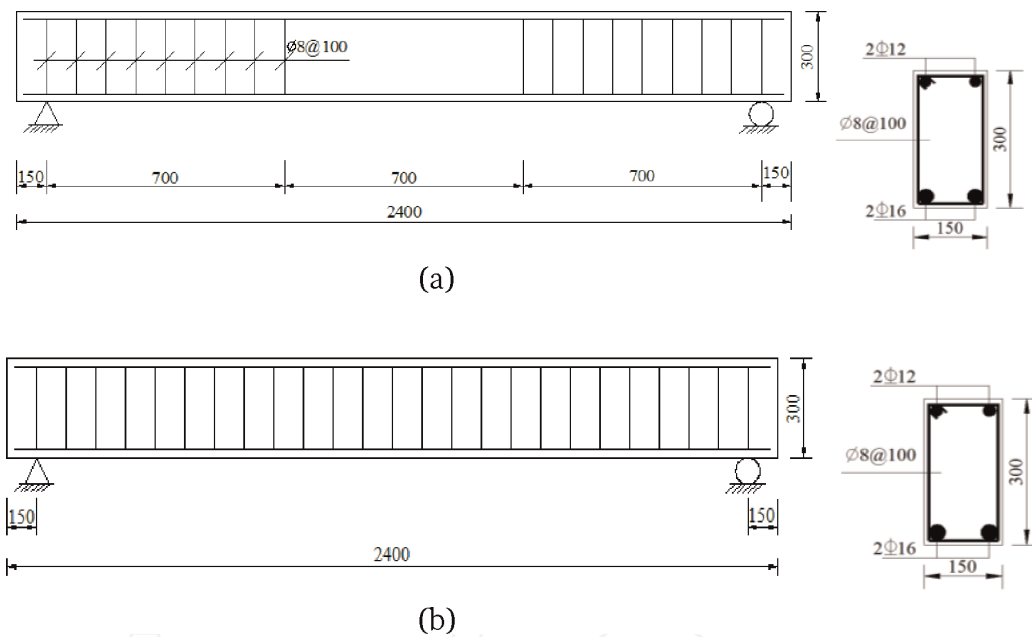
No.	$f_t$ (MPa)	$f_y$ (MPa)	$A_{sv}$ (mm <sup>2</sup> )	$\lambda$	$h_0$ (mm)	$b$ (mm)	$V_{cs}^c$ (kN·m)	$V_{cs}^t$ (kN·m)	$V_{cs}^t/V_{cs}^c$
-----	-------------	-------------	-----------------------------	-----------	------------	----------	-------------------	-------------------	---------------------

S4	1.56	316	100.5	2	267	150	91.81	93.55	1.02
S5	1.50	316	100.5	2	270	150	91.62	92.65	1.01
S6	1.59	316	100.5	2	265	150	91.71	94.83	1.03
S7	1.64	316	100.5	0.95	267	150	111.09	103.75	0.93
S8	1.53	316	100.5	1.5	267	150	97.33	97.05	1.00
S9	1.58	316	100.5	3.05	267	150	84.00	85.35	1.02
S10	1.62	316	100.5	2	267	150	93.01	99.30	1.07
S11	1.54	316	100.5	2	267	150	115.63	118.75	1.03
S12	1.57	316	100.5	2	267	150	78.55	82.3	1.05

Notes: (1)  $f_t$  stands for axial tensile strength obtained by the test or calculated directly by splitting tensile strength or bending strength; (2)  $M_u^c$  and  $M_u^t$  stand for the ultimate bending moment of the normal section calculated by the code and the test values, respectively; (3)  $V_{cs}^c$  and  $V_{cs}^t$  stand for the ultimate shear strength of the diagonal section calculated by the code and the test values, respectively.

**Table 25.**

Theoretical and test values of ultimate strength for normal and diagonal sections, respectively.

**Figure 5.**

Sketch of reinforcement for bending and shear beams, respectively. (a) Sketch of reinforcement for bending beam, and (b) Sketch of reinforcement for shear beam.

## 7. Properties of lightweight sand mortar

### 7.1 General performance of mortar

Because of the rough surface and higher porosity, SP can absorb cement particles and water, which leads to poor mixture workability, so an admixture of cellulose ether, emulsion powder, and so on must be added to meet the code requirements for the mortar consistency and delamination degree of mortar [18–20]. The mix proportions for different strength grades and the test results are shown in **Table 26**.

Compared with the code [18, 19], the dry apparent density of lightweight sand mortar is smaller than  $1900 \text{ kg/m}^3$ , and the heat conduction coefficient is smaller than  $0.8\text{--}1.0 \text{ W/(m}\cdot\text{K)}$ . Because of the porosity of SP, the dry apparent density and heat conduction coefficient are smaller than those of normal-weight sand mortar, so SP has better thermal insulation performance.

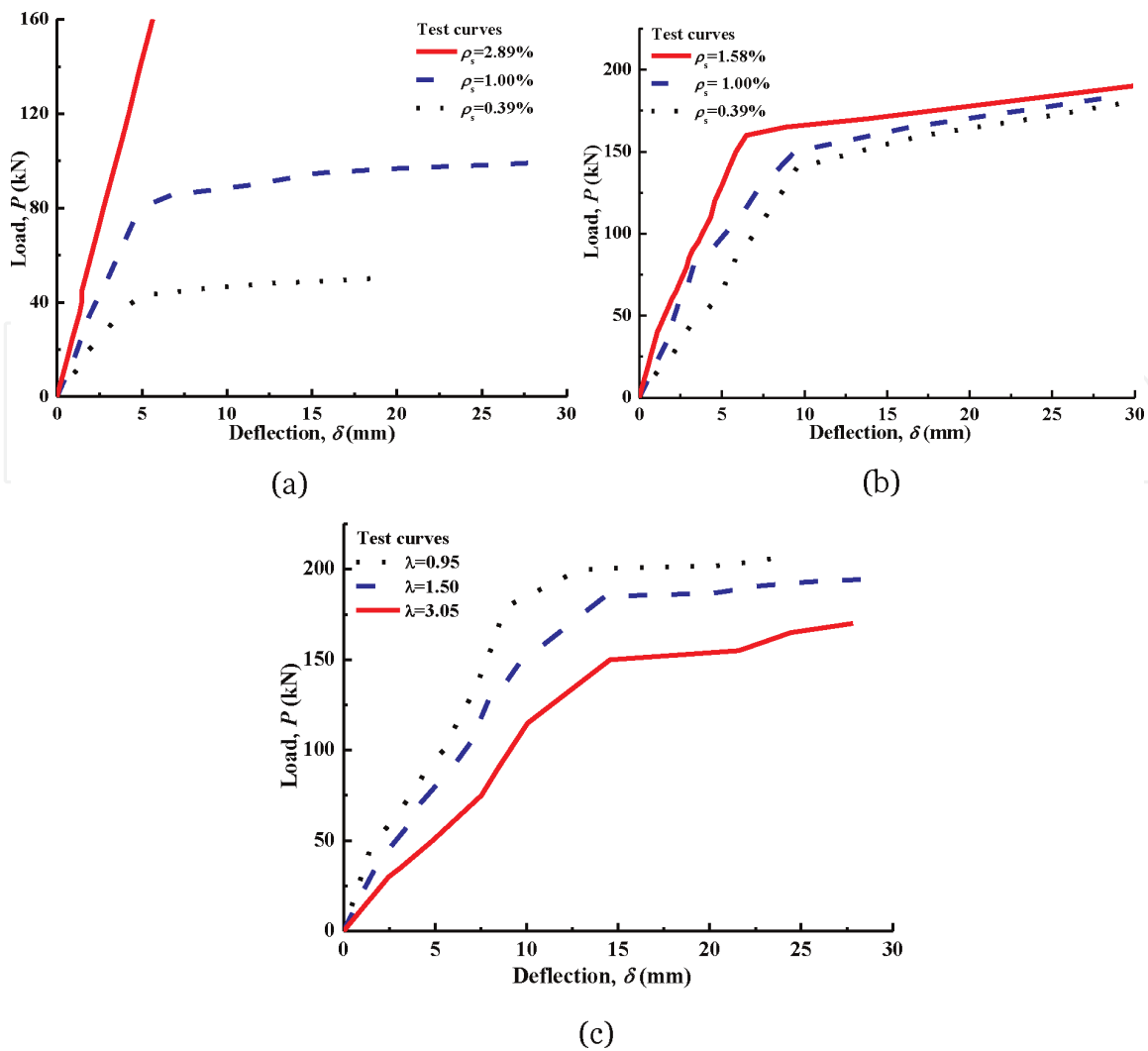


**Figure 6.**  
 Test curves for load deflection. (a) Bending beam, (b) Shear beam, and (c) Shear beam.

## 7.2 Durability of mortar

Taking carbonisation, chloride iron penetration, and sulphate attack, for example, the test results are shown in **Table 27**.

The durability of mortar is enhanced with increases in the strength grade. Especially until 30 cycles, the mass increases. Analogously, the sulphate resistance coefficient is also enhanced until 15 cycles. The reason for this is the porosity and water absorption capacity of SP, which can strengthen the internal curing capacity and thus promote the hydration reaction.

## 7.3 Fire-resistant performance of mortar

The test results for cubic compressive strength, tensile bond strength, and heat conduction coefficient after elevation of the temperature are shown in **Table 28**, where the average values of mass loss are 9, 19, 39, 53, and 65 g after 100, 200, 300, 400, and 500°C, respectively.

The behaviour of the mortar is similar to that of concrete after the elevation of temperature, and the residual strengths after high-temperature treatment are almost 75% at 500 °C and can therefore meet the fire protection design requirements. Below 300°C, the strength and heat conduction coefficient increase; however, at temperatures above 300°C, the strength and heat conduction coefficient decrease, and all of the parameters increase with increases in the strength grade.

Strength grade	$m_C$ (kg)	$m_{FA}$ (kg)	$m_{SP}$ (kg)	$\omega_{EP}$ (%)	$\omega_{CE}$ (%)	$m_W$ (kg)	MC (mm)	DM (mm)	$f_{cu}$ (MPa)	$f_{tb}$ (MPa)	$\lambda$ ( $w \cdot m^{-1} k^{-1}$ )	$\rho_d$ ( $kg/m^3$ )
LM 5.0	162	28	880	1.75	0.35	285	77	12	6.0	0.2319	0.2432	1132
LM 7.5	184	32				273	76	14	7.9	0.3163	0.2762	1217
LM 10	206	35				260	79	9	12.4	0.5135	0.2777	1188
LM 15	251	43				260	82	10	17.2	0.5802	0.2982	1273
LM 20	296	51				248	76	9	22.5	0.5781	0.3190	1348

Notes: (1)  $\omega_{EP}$  and  $\omega_{CE}$  are the emulsion powder (EP) and cellulose ether (CE) content (mass) of cement, respectively; (2) MC and DM stand for the mortar consistency (MC) and delamination degree of mortar (DM), respectively; (3)  $f_{tb}$  stands for the tensile bond strength; (4)  $\lambda$  stands for the heat conduction coefficient.

**Table 26.**  
Reference mixes ( $1 m^3$ ) and test results of lightweight sand mortar.

Strength grade	$h_c^{28\text{ d}}$ (mm)	$Q_c^{56\text{ d}}$ (C)	Mass loss (g)			Corrosion resistance coefficient (%)		
			$\Delta m^{15}$	$\Delta m^{30}$	$\Delta m^{60}$	$K_f^{15}$	$K_f^{30}$	$K_f^{60}$
LM 5.0	19.42	1042.3	18.1	20.2	-12.1	130	78.4	40.8
LM 7.5	18.32	902.4	16.3	19.6	-10.9	128	79.8	55.7
LM 10	18.01	858.4	16.5	17.7	-9.4	125	83.9	68.4
LM 15	17.65	743.8	15.5	16.9	-8.5	120	85.3	71.1
LM 20	15.13	701.2	13.8	15.1	-7.7	119	91.4	75.6

**Table 27.**  
 Test results for durability of lightweight sand mortar.

	$T$ (°C)	LM 5.0	LM 7.5	LM 10	LM 15	LM 20
$f_{cu}$ (MPa)	100	6.5	8.3	12.9	18.0	23.4
	200	7.1	9.2	13.8	18.7	24.1
	300	7.8	10.3	14.9	18.9	24.7
	400	5.7	7.6	11.2	16.0	20.4
	500	4.7	6.3	9.2	14.3	18.7
$\eta_{cu}^T$ (%)	500	78.3	79.7	74.2	83.1	83.1
$f_{tb}$ (MPa)	100	0.100	0.146	0.349	0.366	0.397
	200	0.114	0.160	0.420	0.468	0.510
	300	0.123	0.175	0.430	0.504	0.532
	400	0.090	0.117	0.308	0.328	0.348
	500	0.083	0.106	0.170	0.214	0.239
$\lambda$ ( $\text{w}\cdot\text{m}^{-1}\text{ k}^{-1}$ )	100	0.231	0.253	0.260	0.275	0.299
	200	0.211	0.239	0.248	0.259	0.277
	300	0.220	0.241	0.253	0.263	0.281
	400	0.205	0.226	0.230	0.241	0.259
	500	0.204	0.218	0.222	0.236	0.254

**Table 28.**  
 Strength and heat conduction coefficient of lightweight sand mortar after elevated temperature treatment.

## 8. Summary

ALWC has a number of advantages and disadvantages. Using NS (or MS) and crushing stone to replace a part of LWAs alone or at the same time in equal volume ratio, the new concrete types can be called semi-lightweight concrete (semi-LWC), which includes SLWC, GLWC, HALWC, and so on. Semi-LWC can not only reduce the cost of ALWC but also increase the properties of ALWC, such as workability, strength, durability, anti-deformation, fire resistance, and so on. Especially, moderate amounts of mineral powder and limestone powder can significantly increase the strength and durability.

All types of the concrete can meet the Chinese National Code requirements as well as have a smaller heat conduction coefficient and higher ratio of cubic compressive strength to dry apparent density than NWC. However, the effect of NWAs on semi-LWC is different. Gravel aggregates are bigger than sand aggregates, so the effect is more complex when added simultaneously. At the same time, the multiaxial strength increases with increasing lateral pressure, and the ratio of biaxial

compressive strength to uniaxial compressive strength is slightly larger compared to NWC. This is because the NWA has better thermal conductivity and a small quantity of NWAs can help to reduce autogenous shrinkage of ALWC. On the other hand, the axial compressive strength of ALWC is close to cubic compressive strength, which shows that the ALWC has a self-lubricated antifriction effect because of the SC. On the contrary, if the diameter of SC is too large, its TCS is too small. The strength of ALWC decreases with increasing curing age, so the diameter of SC should not exceed 15 mm in general.

Although the SC has a softening effect, the LWACs do not, so they can be used in hydraulic structure engineering. Even the stiffness of the reinforced ALWC is smaller than that of NWC; because of the smaller modulus of elasticity and apparent density, the reinforced ALWC has a better bending and shear properties. Moreover, the maximum width of crack in ALWC is smaller than that in NWC, so buildings made of ALWC can have better anti-seismic properties.

The highest strength grade of foamed concrete made of SC and SP can be up to LFC 30, so it can be used in non-structure and structure construction, and it has better performance in terms of thermal resistance, sound absorption, insulation, fire resistance, and so on. On the other hand, mortar made of SP can also be used in plastering mortar and masonry mortar and has the abovementioned excellent characteristics.

At high temperature, the performances of LWACs and mortar decrease with increasing temperature but can be increased with increasing lateral pressure. In negative-temperature curing within the range of  $-15^{\circ}\text{C}$ , the LWACs can meet the construction requirements of the artificial freezing method.

Finally, it should be pointed out that the descending curve of the stress-strain curve of LWACs cannot be measured easily, especially after elevation of the temperature. Even so, the formulas provided in this paper can meet the demands of experimental precision under both uni- and multiaxial stress states.

## Acknowledgements

This work was financially supported by the National Natural Science Foundation of China (41172317; 51774112; 51474188). This chapter was polished by Proof-Reading-Service.com Ltd.

## Author details

Jianhui Yang

Henan Province Engineering Laboratory for Eco-Architecture and the Built Environment, Henan Polytechnic University, Jiaozuo, PR China

\*Address all correspondence to: yangjianhui@hpu.edu.cn

## IntechOpen

© 2019 The Author(s). Licensee IntechOpen. This chapter is distributed under the terms of the Creative Commons Attribution License (<http://creativecommons.org/licenses/by/3.0>), which permits unrestricted use, distribution, and reproduction in any medium, provided the original work is properly cited. 

## References

- [1] GB/T 14684–2011. Sand for Construction. China; 2011 (in Chinese)
- [2] GB/T 17431.1-2010. Lightweight Aggregates and its Test Methods—Part 1: Lightweight Aggregates. China; 2010 (in Chinese)
- [3] JGJ/T 241-2011. Technical Specification for Application of Manufactured Sand Concrete. China; 2011 (in Chinese)
- [4] JGJ 52-2006. Standard for Technical Requirements and Test Method of Sand and Crushed Stone (or Gravel) for Ordinary Concrete. China; 2010 (in Chinese)
- [5] GB/T 50266-2013. Standard for Test Methods of Engineering Rock Mass. China; 2013 (in Chinese)
- [6] GB 50496-2009. Code for Construction of Mass Concrete. China; 2009 (in Chinese)
- [7] Taylor MA, Jain AK, Ramey MR. Path dependent biaxial compressive testing of an all-lightweight aggregate concrete. *Automation (Cleveland)*. 1972;**69**(12): 758-764
- [8] JGJ 51-2002. Technical Specification for Lightweight Aggregate Concrete. China; 2002 (in Chinese)
- [9] GB/T 17431.2-2010. Lightweight Aggregates and its Test Methods – Part 2: Test Methods for Lightweight Aggregates. China; 2010 (in Chinese)
- [10] GB/T 50082-2009. Standard for Test Methods of Long-Term Performance and Durability of Ordinary Concrete. China; 2009 (in Chinese)
- [11] Guo Z, Zhang X, Zhang D, et al. Experimental investigation of the complete stress-strain curve of concrete. *Journal of Building Structures*. 1982; **3**(1):1-12 (in Chinese)
- [12] Yang J, Yang Z, Huang H, et al. Multiaxial strength model of concrete. *Engineering Mechanics*. 2008;**25**(11): 100-110 (in Chinese)
- [13] JG/T 266-2011. Foamed concrete. China; 2011 (in Chinese)
- [14] JGJ/T 341-2014. Technical specification for application of foamed concrete. China; 2014 (in Chinese)
- [15] GB/T 50152-2012. Standard for test method of concrete structures. China; 2012 (in Chinese)
- [16] JGJ 12-2006. Technical specification for lightweight aggregate concrete structures. China; 2006 (in Chinese)
- [17] GB 50010-2010. Code for design of concrete structures. China; 2010 (in Chinese)
- [18] JGJ/T 98–2010. Specification for mix proportion design of masonry mortar. China; 2010 (in Chinese)
- [19] JGJ/T 220-2010. Technical specification for plastering mortar. China; 2010 (in Chinese)
- [20] JGJ/T 70-2009. Stand for test method of basic properties of construction mortar. China; 2009 (in Chinese)